

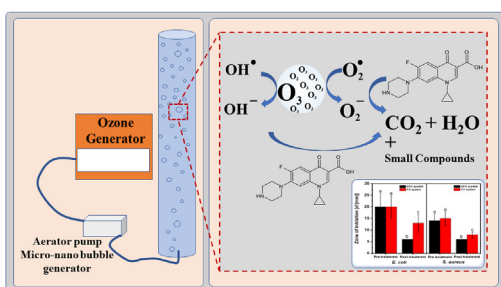


## Research article

## Degradation of ciprofloxacin in aqueous solution using ozone microbubbles: spectroscopic, kinetics, and antibacterial analysis

Sera Budi Verinda<sup>a</sup>, Muflihatul Muniroh<sup>b</sup>, Eko Yulianto<sup>c</sup>, Nani Maharani<sup>d</sup>, Gunawan Gunawan<sup>e</sup>, Nur Farida Amalia<sup>f</sup>, Jonathan Hobley<sup>g</sup>, Anwar Usman<sup>h</sup>, Muhammad Nur<sup>c,f,\*</sup><sup>a</sup> Biomedical Graduate Program, Faculty of Medicine, Universitas Diponegoro, Tembalang, Semarang 50275, Indonesia<sup>b</sup> Department of Physiology, Faculty of Medicine, Universitas Diponegoro, Tembalang, Semarang 50275, Indonesia<sup>c</sup> Center for Plasma Research, Integrated Laboratory, Universitas Diponegoro, Tembalang, Semarang 50275, Indonesia<sup>d</sup> Department of Pharmacology and Therapy, Faculty of Medicine, Universitas Diponegoro, Tembalang, Semarang 50275, Indonesia<sup>e</sup> Department of Chemistry, Faculty of Science and Mathematics, Universitas Diponegoro, Tembalang, Semarang 50275, Indonesia<sup>f</sup> Department of Physics, Faculty of Science and Mathematics, Universitas Diponegoro, Tembalang, Semarang 50275, Indonesia<sup>g</sup> Department of Biomedical Engineering, National Cheng Kung University, No. 1 University Road, Tainan City 701, Taiwan<sup>h</sup> Department of Chemistry, Faculty of Science, Universiti Brunei Darussalam, Jalan Tungku Link, Gadong BE1410, Brunei

## GRAPHICAL ABSTRACT



## ARTICLE INFO

## Keywords:

Ciprofloxacin  
Antibiotic contaminants  
Degradation  
Ozone  
Microbubbles

## ABSTRACT

Ciprofloxacin (CIP) has been listed in the last version of the surface water due to its ability to kill human cells by inhibiting the activity of DNA topoisomerase IV. Thus, CIP, along with other antibiotic pollution has become a serious threat to the environment and public health. Ozonation has been used as an advanced technique that is applied in wastewater treatment to remove CIP, but the primary limitation of this method is the low solubility of ozone in water. This study is the first report of CIP removal in a scale-up of its aqueous solution using a self-developed aerator pump-enhanced ozonation (APO) system, which only employs a propeller and a zigzag arrangement of meshes. This aerator pump decreased the size of ozone bubbles by 90% and increased the effective ozone solubility to 0.47 ppm. The mechanism of degradation of CIP is attributed to an oxidation reaction of the antibiotic with reactive oxygen species, such as hydroxyl, oxygen, and hydroperoxyl radicals, generated on the surface of the ozone microbubbles. It was found that the rate and efficiency of degradation of CIP using the APO system were  $3.64 \times 10^{-3}$ /min and 83.5%, respectively, which is higher compared with those of conventional flow ozonation (FO) systems ( $1.47 \times 10^{-3}$ /min and 60.9%). The higher degradation efficiency of CIP by the APO system was also revealed by its higher electrical energy efficiency (0.146 g/kWh), compared to that of the FO

\* Corresponding author.

E-mail address: [mnur@lecturer.undip.ac.id](mailto:mnur@lecturer.undip.ac.id) (M. Nur).<https://doi.org/10.1016/j.heliyon.2022.e10137>

Received 8 March 2022; Received in revised form 30 May 2022; Accepted 28 July 2022

2405-8440/© 2022 The Author(s). Published by Elsevier Ltd. This is an open access article under the CC BY-NC-ND license (<http://creativecommons.org/licenses/by-nc-nd/4.0/>).

system (0.106 g/kWh). The degradation of CIP was also monitored by the resulting antibacterial activity against *Escherichia coli* and *Staphylococcus aureus*.

## 1. Introduction

Antibiotics have saved millions of lives since their discovery in the 1930s. They are used extensively to improve human health as well as in veterinary practice to treat infectious diseases and to promote growth. These diverse uses have resulted in a steady increase in global antibiotic consumption. The global antibiotic consumption rate was projected to rise from 42.3 billion defined daily doses (DDDs) in 2015 to 128 billion DDDs in 2030, which is equal to an increase of 15.8 DDDs per 1,000 inhabitants each day [1]. Typically, more than 58% of the consumed antibiotics are not metabolized, and they are excreted through urine and feces into the sewerage system and surface waters [2]. Contamination of water bodies with antibiotics is a serious concern due to the proliferation of antibiotic-resistant pathogens [3, 4, 5].

Ciprofloxacin [CIP;  $C_{17}H_{18}FN_3O_3$ ] (Figure 1) is one of the reported antibiotic pollutants found in aquatic environments [6, 7]. CIP is the second generation of fluoroquinolone antibiotics and has a broad spectrum of pharmaceutical and biological activity. This antibiotic kills bacterial cells by inhibiting the catalytic activity of DNA gyrase and topoisomerase IV enzymes during replication and transcription [8]. CIP can also interact with human DNA topoisomerase II [9], and therefore has the potential to kill various human cells [10]. CIP tends to accumulate in aquatic environments, due to its low biodegradability, eventually leading to high concentrations [11, 12]. CIP can also disperse into the foodchain via trophic transfer [13, 14, 15, 16, 17]. In addition, a sub-inhibitory dose of CIP may lead to the development of resistance to antimicrobial drugs, therefore it poses threats to both environmental and human health [18].

Due to the problems outlined above, an effective treatment to remove CIP and other antibiotics from wastewater is long overdue. Biological treatment is the conventional method used to remove antibiotics in general in wastewater treatment plants (WWTPs). However, this method is inefficient at removing antibiotics based on fused aromatic rings, such as CIP [2, 19, 20]. Moreover, some studies have reported that WWTPs cannot remove recalcitrant organic compounds (ROCs). This means that the treatment plants require the use of a large amount of energy and use an excessive amount of oxygen [21]. Because of this, CIP was found at concentrations of 28–31 mg/L in the effluent of a pharmaceutical manufacturing unit [22] and was even reported to be as high as 6.5 mg/L in two Brazilian lakes [23, 24].

The application of advanced oxidation processes (AOPs), which employ either ozone microbubbles, UV light, or catalysts, have been reported as promising methods for oxidative removal of various organic contaminants in polluted water [25]. The basic principle of AOPs is that they generate reactive oxygen species (ROS), including hydroxyl ( $OH^{\bullet}$ ),

oxygen ( $O_2^{\bullet-}$ ), and hydroperoxyl ( $HO_2^{\bullet}$ ) radicals on the surfaces of ozone microbubbles or catalysts [26]. For AOPs, the amount of oxidizing agent required depends mainly on the volume of effluent and the concentration of contaminants to be removed. Typically the volumes and concentrations can be high, therefore the use of electrochemical methods are inefficient and the use of complex chemical oxidizing agents is considered inappropriate [22, 27, 28, 29], because they need high surface area of the electrode and the use of excessive oxidizing agents merely increases the operational cost and the amount of toxic waste.

Among the AOP-based methods, dielectric barrier discharge plasma (DBDP) is an efficient green technology for the degradation of antibiotics [22, 26, 30, 31]. However, DBDP has high operational costs, making it impractical for industrial process scale-up [32]. This is unfortunate because DBDP is more effective than UV light-based AOP, which needs to be used in combination with other treatments in order to achieve a useful oxidizing efficiency [33, 34, 35]. Another limitation of DBDP is that the ozone that it produces has low solubility in water with a Henry's law solubility constant ( $H^{CP}$ ) of  $1.0 \times 10^{-6}$ – $1.3 \times 10^{-4}$  mol/m<sup>3</sup>.Pa [36]. This results in a low mineralization capability. Therefore, ozone production on its own is inadequate for the treatment of persistent contaminants in wastewater. This problem could be overcome by flowing the ozone into the wastewater in the form of microbubbles and nanobubbles using a simple aerator pump. Ozone microbubbles and nanobubbles have a low Rayleigh number in water [37], allowing them to rise slowly toward the water surface [38], so they can remain dispersed in the wastewater for a longer time. This increases the probability that organic contaminants will react with ROS produced on the surface of the ozone microbubbles and nanobubbles [39, 40, 41].

The present study aims to analyze the following:

- (i) The concentration of dissolved ozone in an aqueous solution produced using either aerator-pump-based ozonation (APO) or diffused flow ozonation (FO) systems.
- (ii) The efficiency of CIP degradation by the resulting ozone microbubbles.
- (iii) The pseudo-first order kinetics of the process based on spectroscopic data.
- (iv) The effectiveness of the APO and FO systems, in terms of the degradation efficiency and electrical energy consumption.
- (v) The residual environmental hazard of the treated CIP waste, evaluated from the antibacterial activity against *Escherichia coli* and *Staphylococcus aureus* bacterial strains.

This study uses a scaled up volume of CIP solution (10 L), which is challenging, because a larger volume makes it harder to disperse the ozone. This is the first report of scaled-up removal of CIP solution using ozone microbubbles. One of the challenges that is addressed is the limited availability of advanced quantification tools, such as ultra-high performance liquid chromatography, high-performance liquid chromatography, and liquid chromatography-mass spectroscopy. The solution provided in this study was to quantify the degradation of CIP using a simple UV-Vis spectrophotometer which could adequately provide quality control analyses. The successful application of the method was further confirmed by antibacterial studies on the treated CIP waste-stream.

## 2. Experimental

### 2.1. Materials

Ciprofloxacin (1-Cyclopropyl-6-fluoro-4-oxo-7-(piperazine-1-yl)-1,4-dihydro-quinoline-3-carboxylic acid, CAS# 85721-33-1, Sigma Aldrich,

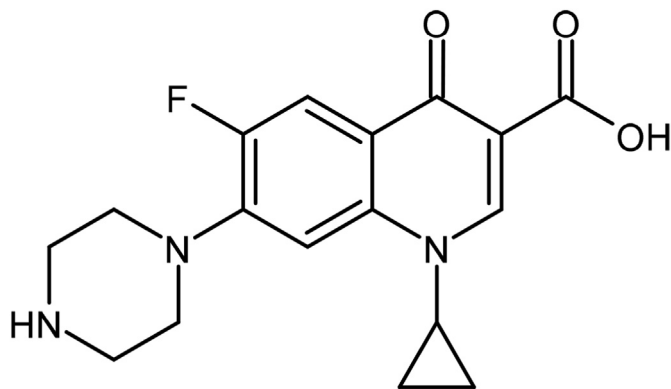


Figure 1. The chemical structure of ciprofloxacin.

17850), methanol (Merck, 106009), potassium iodide (KI, Merck, 105043) and sodium thiosulfate ( $\text{Na}_2\text{S}_2\text{O}_3$ , Merck, 106516) were purchased from Merck (Darmstadt, Germany) and used without further purification. A 1.000 mg/L stock solution of CIP was prepared in methanol. The stock solution was further diluted 100 $\times$  in ultrapure water [pH 7, and resistivity 19.8 MO.cm (Milli Q Integral 5 purification system; Millipore, USA)] to obtain a 10 mg/L solution of CIP as a simple model of wastewater contaminated by antibiotics. This pure water was free from trace elements or natural organic matter, while organic carbon (OC) was 2.7 ppm. No pH changes were observed in the CIP solutions before and after dilution in any of the experiments performed.

## 2.2. Ozone generator

Ozone was generated using a DDBD plasma generator, which consists of two Pyrex glass barriers separated from each other by 3 mm [42, 43]. This type of DDBD is known to generate high purity ozone, because the barriers keep the electrodes free from corrosion preventing contamination [43]. Pure oxygen was used as a feed-gas source. The volumetric flow rate of the oxygen gas into the generator was set to be 0.3 L/min, while the voltage discharge applied to the DDBD was 3 kV.

## 2.3. Ciprofloxacin treatment and sampling methods

10 L of CIP solution was placed inside an open acrylic tube with dimensions of  $37 \times 24 \times 15 \text{ cm}^3$ . Ozone, which was generated by DDBD plasma generator, was injected into this solution continuously for 600 min. Ozone was injected either through diffused-ozonation using a stone diffuser ( $d = 1.2 \text{ cm}$  and  $h = 2.9 \text{ cm}$ ) or through an enhanced-ozonation method employing an aerator pump which provided a pressurized dissolution to generate microbubbles, as schematically shown in Fig. S1. This aerator pump has a propeller that is perpendicular to both the ozone intake [44, 45] and the flow direction of the CIP solution (Fig. S2). The volumetric flow rate of the CIP solution was 50 L/min, while the propeller rotated this solution at higher speed, so that the pressure of flowing solution was much lower than the pressure of inlet ozone around the propeller. This is known as a cavitation phenomenon and produces ozone microbubbles. The comparative degradation efficiency of CIP was then investigated using conventional ozonation and using the ozone microbubbles.

The degradation of CIP in the acrylic tube was monitored every 30 min. To achieve this, 4 mL aliquots of the CIP solution were taken from a depth of 3 cm below the surface using a 5 mL plastic syringe at five different locations (Fig. S1c). This was repeated for five different observation sites. The total volume of CIP solution collected from each monitoring time before and after ozone microbubble treatment was 100 mL. This sampled solution was stored in an amber glass bottle covered with aluminum foil. The solutions were kept at 4 °C for further antimicrobial activity tests. All of these experiments were performed in duplicate.

## 2.4. Ozone concentration and dissolution measurement

The concentration of ozone generated ( $C_{O_3}$ ) by the DDBD plasma generator was measured using the iodometric titration method following procedures that have been previously reported [46]. Briefly, the output ozone was injected into 50 mL of KI solution (0.2 M) for 3 min. The injected ozone oxidizes  $\text{I}^-$  ions to form  $\text{I}_2$  molecules, which gives a yellow to brown color to the initially clear KI solution. This ozonated KI solution was then titrated with  $\text{Na}_2\text{S}_2\text{O}_3$  solution (0.4 M) until it became clear again. The volume of spent  $\text{Na}_2\text{S}_2\text{O}_3$  solution was measured to calculate the output concentration of ozone ( $C_{O_3}$ ) [46]. The output ozone capacity ( $K_{O_3}$ ) was then calculated by multiplying the value of  $C_{O_3}$  by the flow rate ( $V_{O_2}$ ). Both of  $C_{O_3}$  and  $K_{O_3}$  were measured several times during the

experiments to ensure the reproducibility and stability of the DDBD ozone generator.

Although, there is no a standard method to measure ozone dissolution in water, in this study, ozone dissolution was measured using a colorimetric method (Spectroquant<sup>®</sup> MoveDC Mobile Colorimeter, Merck, 173635), which was set to have the largest measurement range. The generated ozone was continuously injected into 10 L distilled water for 120 min. About 4 mL of the ozonated distilled water was taken every 10 min. This was repeated three times. Thus, the dissolved ozone concentration ( $C_{DO_3}$ ) was measured in triplicate. Unlike the measurement of  $C_{O_3}$  and  $K_{O_3}$ , the measurement of  $C_{DO_3}$  was performed only during the optimization experiment. The highest  $C_{DO_3}$  value obtained from optimization experiment was assumed to be a reliable parameter to determine the optimum operational conditions such as the voltage (V) and the flow rate of oxygen inlet ( $V_{O_2}$ ).

## 2.5. Quantification of bubble characteristics

The diameters of microbubbles generated through the aerator pump were measured based on images captured using a digital single-lens reflex camera (Canon EOS 70D) operating with a lens aperture of  $f/9$ , a shutter speed of 1/3200 s and ISO of 12800. The focus was set at 2 cm above the output nozzle of the aerator pump (Fig. S3). With this setup, the expected minimum diameter of ozone microbubbles captured by the digital camera was approximately 12.0  $\mu\text{m}$ . The captured images were processed using ImageJ software to produce quantitative data on bubble diameters [47]. For this analysis a 24-bit uncompressed-color image was converted to an 8-bit gray-scale image. In the images, circles with a solid white border were then identified as in-focus ozone microbubbles. The image of an object with a known diameter was used as a standard to verify the conversion factor from pixel units to a physical dimension unit (Fig. S4). This calibration was applied to all of the captured images. The dimensional analysis of the bubbles was carried out by quantifying a selected area of  $2 \times 1.5 \text{ cm}^2$  from the original image.

## 2.6. Quantification of ciprofloxacin concentration

The concentration of the CIP solution before and after being treated with ozone microbubbles was quantified based on its absorption spectrum, which was measured in 1-cm standard cuvette cell using a UV-visible spectrophotometer (Genesys 150, Thermo Scientific, USA). The absorption spectra were recorded at slow scan rate with a spectral range from 200 nm to 600 nm. Prior to every measurement, the cuvette was cleaned by rinsing three times with distilled water, then dried. A standard calibration curve was made of absorbance as a function of CIP concentration, in the range of 1–19 mg/L. 1% v/v methanol was used as blank solution during this quantification. The  $R^2$  values of linear regression of the calibration curves at 287, 322, and 333 nm were 0.967, 0.992, and 0.992, respectively, as shown in Fig. S5. The peak at 322 nm was chosen to determine the concentration of CIP, because this peak had the highest linearity determinant and molar extinction coefficient.

The degradation efficiency ( $\eta\%$ ) and the electrical energy efficiency ( $E_{\text{eff}}$ ) of CIP upon ozone microbubble treatment were calculated from the experimental data using Eqs. (1) and (2), respectively [48, 49]:

$$\eta = \frac{C - C_0}{C_0} \times 100 \quad (1)$$

$$E_{\text{eff}} = \frac{(C_0 - C) \times V_0}{P \times t \times 60} \quad (2)$$

where  $C_0$  is the initial concentration of CIP in the solution (mg/L),  $C$  is the remaining concentration of CIP after a given treatment time  $t$  (min),  $V_0$  is the volume of aqueous solution of CIP (L),  $P$  is the electrical power (W).

## 2.7. Quantification of organic carbon

The Walkley-Black method was used to quantify the concentration of OC in the sample during ozonation [50, 51]. The organic matter (OM) existing in the sample was oxidized by a mixture of 0.4 N potassium dichromate ( $K_2Cr_2O_7$ ) and concentrated sulfuric acid ( $H_2SO_4$ ). The remaining chromate was then quantified based on the absorbance of the solution mixture at 600 nm. This method calculates oxidizable organic matter based on organic matter containing 58% carbon.

## 2.8. Disk diffusion assay

A standard disk diffusion assay was employed to determine the antibacterial activity of CIP against *E. coli* and *S. aureus*. The disk diffusion assay was performed according to the guidelines of The European Committee on Antimicrobial Susceptibility Testing (2021) [52]. Each bacterium was inoculated in tryptic soy broth (TSB, Merck 1054590) and it was then incubated overnight at 37 °C. The density of each culture was adjusted to be 0.5 McFarland standard using  $BaCl_2$  and  $H_2SO_4$ . The resulting cell suspensions were further used for inoculation of tryptic soy agar (TSA, Merck 1054585007), and 20  $\mu$ L aliquots of the cell suspensions were deposited on sterile discs (Oxoid CT-0998B). The sterile discs were dried in a laminar flow and placed on inoculated TSA dishes, followed by incubation for 24 h at 37 °C. After the incubation, the zone of bacterial growth inhibition produced on the disks was measured and the diameter was expressed in mm (see Fig. S6). This experiment was performed in triplicate and replicated three times, and the inhibition diameter was presented as the average value of nine measurements.

## 2.9. Broth microdilution

The broth microdilution method was used to determine the minimum inhibitory concentration (MIC) of CIP solution, before and after being treated with ozone microbubbles, against *E. coli* and *S. aureus*. This broth microdilution method was done by adapting the protocol reported by Wiegand et al. [53] and Sarangapani et al. [54]. TSB alone and TSB + bacterial cells were used as a negative control and a positive control, respectively. The concentration of treated CIP was varied to be within 0.001–50% (see Fig. S7). The lowest antibiotic concentration that inhibited the growth of the microorganism was detected by the lack of visual turbidity (matching the negative control) and was determined as the MIC value. This experiment was carried out in triplicate and repeated twice and thus, the MIC value was an average of six measurements.

## 3. Results and discussion

### 3.1. The size distribution of microbubbles

The images captured by a digital camera show that ozone microbubbles are nearly spherical. There were 34 microbubbles (out of 94 bubbles) in the sampling area in the APO system, which is higher compared with the FO system (0 microbubbles out of 49 bubbles). As shown in Figure 2A and B the diameter of the microbubbles was between 62 to 306  $\mu$ m in the APO system, which is much smaller compared with that in the FO system (in the range of 109–2719  $\mu$ m). Fitting the size distribution with a Gaussian function revealed that the peak of size distribution was 108 and 1170  $\mu$ m for the APO and FO system, respectively. It is clearly observed that the average size of microbubbles generated through the APO system is about 10-fold smaller than those produced by the FO system. Therefore, this simple cost-effective aerator pump could successfully improve the cavitation properties, increasing the population of small-sized ozone microbubbles by up to 39% compared to the diffusion system. One may therefore expect that the higher population of ozone microbubbles would play a significant role in increasing the availability and resupply of solvated ozone in water, leading to enhanced degradation of CIP. This finding has favorable implications for cost effective wastewater management.

### 3.2. Concentration of ozone and dissolved ozone microbubbles

After ozonation using the DDBD, the  $C_{O_3}$  was found to be 1.92 g/L. The highest  $K_{O_3}$  value for the APO and FO systems was 28.16 and 34.56  $g\ h^{-1}$ , respectively. Both  $C_{O_3}$  and  $K_{O_3}$  increased to 2.35 g/L and 42.24 g/h in APO and FO systems. Fortunately, there was no significant difference for the value of  $C_{O_3}$  and  $K_{O_3}$  ( $p > 0.05$ ) between the two systems. These data showed that the ozone generator provided good reproducibility and stability.

The time-dependent  $C_{DO_3}$  values achieved by the APO and FO system are shown in Figure 3A, emphasizing that the APO system provides higher  $C_{DO_3}$  values than the FO system. The  $C_{DO_3}$  values were then fitted with the Boltzmann equation, as this equation is known to give the most satisfactory results in interpreting the solubility of ozone in water [55]. The  $R^2$  values of the best fits of the Boltzmann equation on the experimental data are 0.935 and 0.943 for the APO and the FO system, respectively. The best fitting lines revealed that the APO system reaches saturation at 20 min, which is faster than the FO system (40 min), as shown in Figure 3B. The highest  $C_{DO_3}$  value in distilled water for the APO

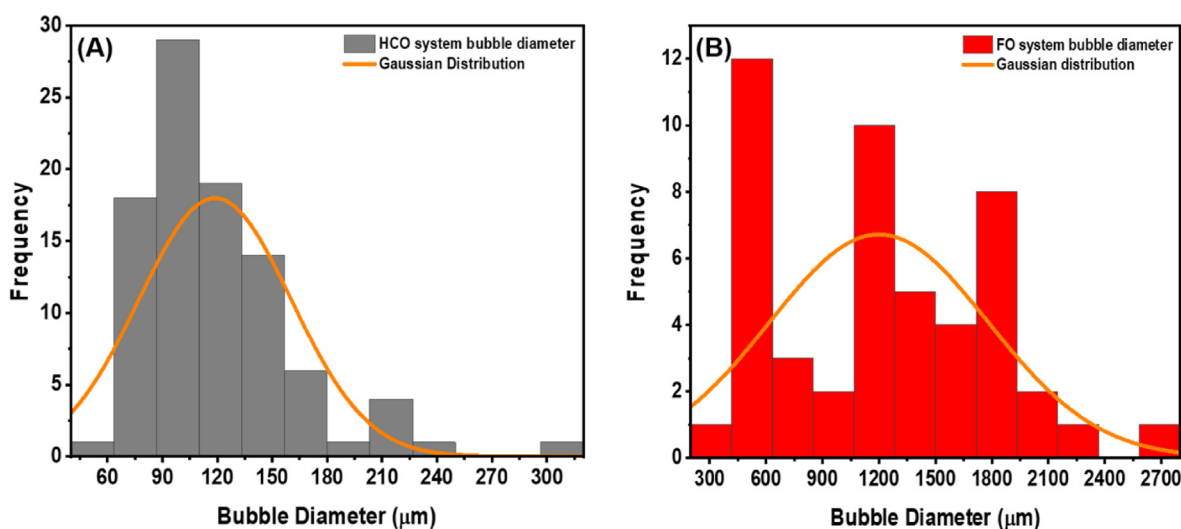
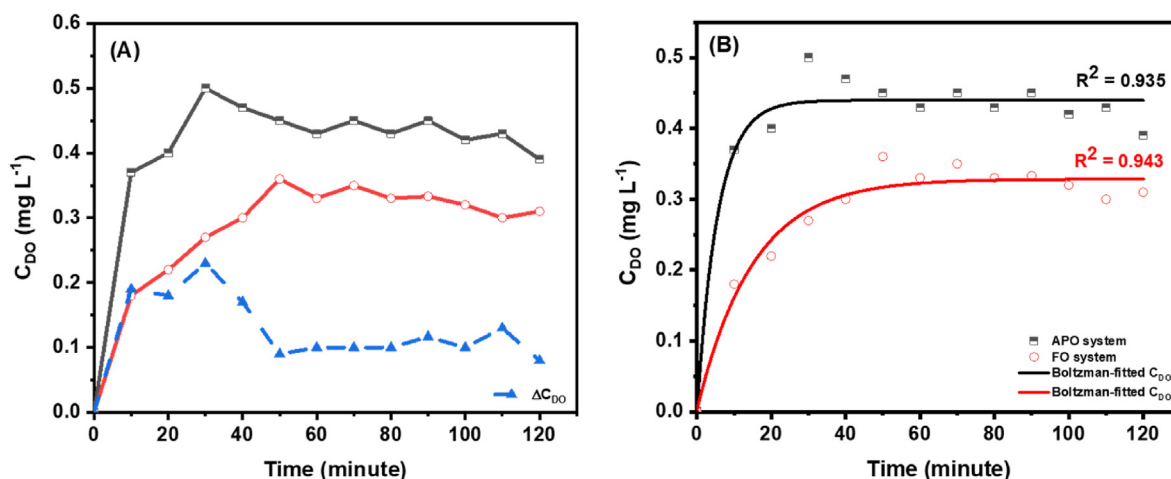


Figure 2. The size distribution of ozone microbubbles the aqueous solution produced through (A) the APO system and (B) the FO system.



**Figure 3.** (A) Plots of the dissolved ozone concentration ( $C_{D0}$ ) in distilled water generated in the APO system (black square), in the FO system (red circle), and the difference of  $C_{D0}$  between the two systems (blue triangle) against time, and (B) the best fit of Boltzmann equation to the experimental data.

and FO systems was 0.43 and 0.31 mg/L, respectively. The difference in the saturation level of  $C_{D0}$  is attributed to the smaller size and the longer persistence of the ozonated microbubbles in the water generated by the APO system as compared to the FO system (see Figure 2).

The generation of ozone microbubbles and nanobubbles using such an aerator pump has been reported in several studies [56, 57, 58]. It has been pointed out that the volumetric flow rate of gas is the most influential parameter for the efficiency of ozone microbubble production [59]. In this study, the flow rate used to generate ozone microbubbles was set based on our optimization study on different flow rates of gas. It was demonstrated that the aerator pump could increase the population of small-sized ozone microbubbles, compared with those produced using a stone diffuser. However, the concentration of dissolved ozone,  $C_{D0}$ , was saturated, similar to the findings reported by Yao et al. [40], though the current  $C_{D0}$  value is far below the reported ozone solubility [59]. The main limitation is the lack of an acceptable standard technique in quantifying  $C_{D0}$  [60]. Thus, the reported  $C_{D0}$  values tend to differ from each other depending on the quantification method. Ozone also rapidly decomposes into a various reactive oxygen species (ROS) after being injected into wastewater [61]. Therefore, many studies have stated that  $\text{OH}^{\bullet}$ ,  $\text{O}_2^{\bullet-}$ , and  $\text{HO}_2^{\bullet}$  radicals play key roles in degrading pollutants in wastewater, rather than ozone itself [26, 54, 62]. In other words, ozone microbubbles in aqueous solution generate various radicals which then oxidize the organic compounds and antibiotics, including CIP [26, 63]. In this case, the solubility of ozone mediates the formation of ROS, especially  $\text{OH}^{\bullet}$ ,  $\text{O}_2^{\bullet-}$ , and  $\text{HO}_2^{\bullet}$  radicals.

The pH and temperature of the CIP solution remained unchanged during the ozone treatment, as shown in Fig. S8. A similar finding has been reported by Wang et al. [59]. In this study, the pH of the CIP solution was stable, which is most likely due to the large volume of the CIP solution, for which slight changes in the amount of  $\text{H}^+$  and  $\text{OH}^-$  ions would not affect the acidity of the solution. In contrast, Sarangapani et al. reported that the pH of their solution decreased when using a small volume of CIP solution [54]. In other words, in a larger volume of CIP solution, the chance of ROS formation by interactions between ozone and  $\text{H}_2\text{O}$  molecules should be higher, but at the same time ozone decomposition processes would be accelerated. Considering the mechanism of ozone dissolution in water and the pH characteristic of the solution in this study, it is conceivable that ozone decomposition might produce a lot of hydroperoxyl ( $\text{HO}_2^{\bullet}$ ) and  $\text{O}_2^{\bullet-}$  radicals [the oxidation potential ( $E_0$ ) = 1.65 V and 1.23 V, respectively]. The efficiency of  $\text{HO}_2^{\bullet}$  radical generation in the CIP solution is inversely proportional to the number of  $\text{OH}^{\bullet}$  radicals because the  $\text{HO}_2^{\bullet}$  and  $\text{O}_2^{\bullet-}$  radicals are generally formed after  $\text{OH}^{\bullet}$  radical decomposition ( $E_0 = 2.80$  V). The formation of  $\text{HO}_2^{\bullet}$  and

$\text{O}_2^{\bullet-}$  radicals is believed to reduce the oxidation potential of organic contaminants in wastewater [32, 61]. The relatively small proportion of  $\text{OH}^{\bullet}$  radical under this scenario could be another reason for the stability of pH of the CIP solution treated by ozone microbubbles even after 600 min. As the pH stability of the CIP solution was observed in both the APO and FO systems, one could consider that the proportion of ROS in the two systems was comparable.

### 3.3. Ciprofloxacin degradation

The time-dependent absorption spectra of CIP solution treated using the APO and FO systems are shown in Fig. S9. Based on these absorption spectra, the respective initial concentrations of CIP ( $C_0$ ) were 10.94 and 11.86 mg/L ( $p > 0.05$ ), while their final concentrations ( $C_f$ ) after treatment with ozone microbubbles generated by the APO and FO systems for 600 min were 1.80 and 4.64 mg/L, respectively. This suggests that the degradation efficiency of CIP treated using the APO system was 83.5%, which is significantly higher than when treated by the FO system (60.9%). The degradation kinetics of CIP were then evaluated by fitting the  $C/C_0$  with a single exponential function with respect to treating time ( $t$ ), as given by Eq. (3) [49, 54];

$$C/C_0 = e^{-kt} \quad (3)$$

where  $C$  is the remaining concentration of CIP in the solution, and  $k$  is the reaction rate constant of CIP degradation by ozonation.

As shown in Figure 4, the degradation kinetic data of CIP in the APO and FO systems were fitted well to a single exponential function with an  $R^2$  of 0.990 and 0.984, respectively, confirming that the degradation of CIP upon ozonation followed the first-order kinetics. This was further confirmed by the linear relationship between  $\ln C/C_0$  as a function of  $t$  ( $R^2 = 0.984$  and 0.970). This finding suggested that the ozone microbubbles can be considered to be rigid bulky materials in the aqueous solution, generating ROS on their surfaces, which accept an electron from CIP, leading to degradation of the antibiotic with pseudo-first-order kinetics [64]. Pseudo-first-order kinetics has also been reported in several studies on the degradation of CIP using photocatalysis [65] and photochemical oxidation [33]. Based on the best fits to a single exponential function over time (see Figure 4), the  $k$  value of CIP degradation upon ozonation injected through the APO system and FO system was  $3.64 \times 10^{-3}/\text{min}$  and  $1.47 \times 10^{-3}/\text{min}$ , respectively. This shows that the degradation of CIP upon ozonation through the APO system was 2.4 times faster than through the FO system. This result can be explained by the higher concentration of dissolved ozone microbubbles in the APO

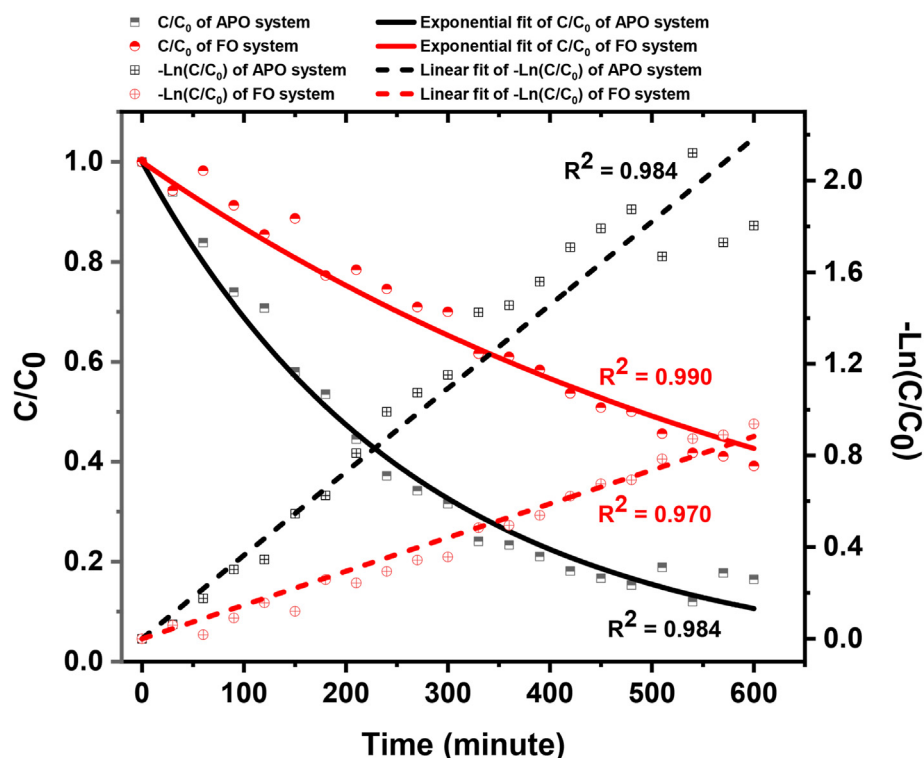


**Figure 4.** The kinetics of ciprofloxacin degradation by ozonated microbubbles generated through the APO system (black square) and in the FO system (red circle). The curve lines represent the best fits of  $C/C_0 = e^{-kt}$ , whereas the linear lines are the best fits of  $-\ln(C/C_0) = e^{-kt}$ , on the experimental data, from which the degradation rate,  $k$ , was deduced.

system compared with that in the FO system, as ozone solubility is proportional to the  $k$  value. In other words, the greater the ozone solubility, the greater the value of  $k$  [20].

The oxidation power of ozone to degrade CIP depends on the number and surface area of ozone microbubbles that can interact with the drug in the wastewater. In this sense, the APO system produces high population and smaller size of ozone microbubbles as compared with the FO system. It is also expected that the small ozone microbubbles will have lower buoyancy and high number density [38], causing the microbubbles to rise more slowly toward the solution surface and allowing the small ozone microbubbles to interact with more CIP molecules for longer via the mass transfer of ozone microbubbles to the wastewater. As a result, the oxidation power of small ozone microbubbles, which can be attributed larger surface area to degrade CIP, is significantly increased.

### 3.4. Organic carbon removal

Mineralization of CIP by ozonation tends to be lower than that of pseudo persistent organic pollutants having only aromatic rings and oxygenated groups [20]. In this sense, the initial concentration of OC in both the APO and FO systems was measured to be 346.7 ppm. In the first 300 min during the treatment, the removal of OC was only about 10% (35 ppm) and 3% (10 ppm) for APO system and FO system, respectively (Figure 5a). These removal efficiencies were significantly lower compared to those of CIP which were 68% for APO system and 30% FO system. This result suggests that OC was not efficiently decomposed in the ozone treatment [66], while CIP degraded through a large number of intermediates which were easily attacked directly by ozone. Such results were previously reported before in several studies [21, 66, 67, 68, 69].

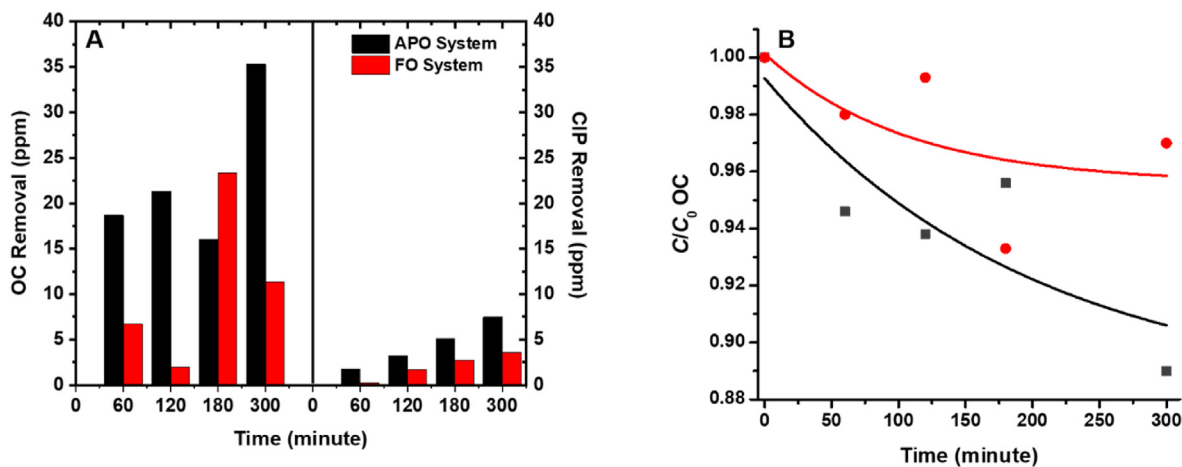


**Figure 5.** (A) The removal of OC (left panel) and CIP (right panel) using the APO system and the FO system, and (B) the plot of  $C/C_0$  of OC treated using the APO system (black squares) and the FO system (red circles) as a function of treatment time and the best fits of single exponential function.

A plot of  $C/C_0$  of OC as a function of treatment time  $t$  is shown in Figure 5b, revealing that concentration of OC decreased nonlinearly, which is similar to CIP. It is noteworthy that the fraction of OC removal was around 10% with respect to its initial concentration, in contrast to ozonation of CIP and amoxicillin in model hospital wastewater, for which 99% removal could be achieved [70]. Although the data points are scattered, fitting them with a single exponential function according to Eq. (3) gave  $k$  values for OC removal upon treated with the APO system and the FO system of  $4.97 \times 10^{-3}/\text{min}$  and  $9.52 \times 10^{-3}/\text{min}$ , respectively.

### 3.5. Electrical energy consumption

As the degradation efficiency of pollutant is related to the energy efficiency, one could estimate either the degradation efficiency of pollutant per unit energy, or the energy consumption per unit mass of degraded pollutant. In this study, the electrical energy consumed by the APO system was measured to be 0.50 kW h, which was higher than that by the FO system (0.38 kWh). However, as mentioned above, the APO system successfully degraded 84% of 10.94 mg/L initial concentration of CIP, while the FO system could only degrade around 61%. Based on these data, the energy consumption analysis showed that the degradation efficiency of CIP per unit electrical energy in the APO and FO systems was 0.146 g/kWh and 0.106 g/kWh, respectively, as shown in Figure 6. This energy consumption analysis unambiguously highlights that the APO system requires lower energy consumption per unit mass of degraded CIP compared with the FO system. As these results indicated that the degradation efficiency of CIP per unit electrical energy of the APO system was 37.7% greater than that of the FO system, it is reasonable to consider that this enhanced energy efficiency could be attributed to the higher population of ozone microbubbles (39%) produced by the aerator pump in the APO system as compared to the conventional diffusion in the FO system. In other words, the introduction of an aerator pump of the APO system, to generate a higher population of ozone microbubbles, added economic value to the ozone injection technology compared with the diffused injection of the FO system. The higher efficiency is most likely due to the burst of microbubbles that can independently generate ROS, aside from ozone-generated ROS [71].

### 3.6. Antibacterial activity

It is interesting to recall that, as CIP is an antibiotic, the degradation of CIP should reduce its antibacterial activity, and this reduction was confirmed in this study. Using a concentration of 10.94 and 11.86 mg/L of CIP, the pre-treatment samples of APO and FO system showed no

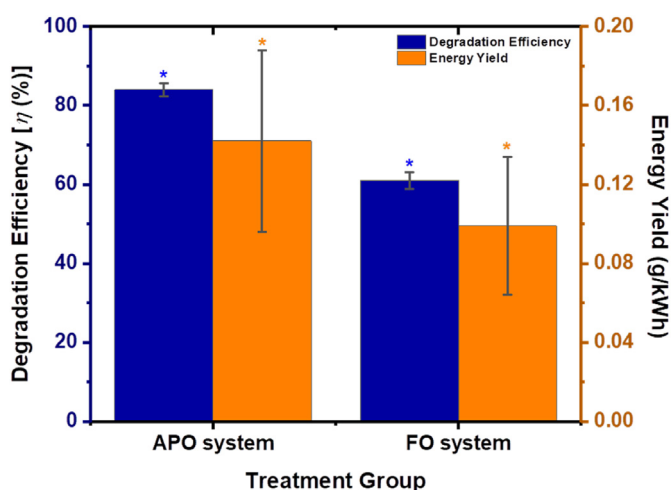


Figure 6. The degradation efficiency of ciprofloxacin,  $\eta$ , (blue histograms) and energy yield (orange histograms) by ozone microbubbles generated through the APO system and in the FO system.

significant difference in antibacterial activity, as the two pre-treated samples exhibited similar inhibition zone, i.e. 20 mm against *E. coli* ( $U = 32$ ;  $p = 0.489$ ) and 14–15 mm against *S. aureus* ( $t_{16} = 0.304$ ;  $p = 0.765$ ), respectively, as shown in Fig. S6. After treatment with ozone microbubbles using the APO system, the inhibition zone decreased to 6 mm for both *E. coli* and *S. aureus* bacterial strains, as shown in Figure 7. These results confirm that the ozone microbubbles in the APO system reduced antibacterial activity of CIP against *E. coli* and *S. aureus* by 14 mm and 8 mm, respectively. These results are higher than that of the ozone microbubbles in the FO system which reduced the antibacterial activity to just 7 and 5 mm against *E. coli* and *S. aureus*, respectively (Tables S1 and S2). However, this disk diffusion assay was not sufficient to explain the antibacterial activity of residual CIP and its decomposition products generated by ozone in the two systems. Thus, the MIC test with a broth microdilution procedure was performed to determine the toxicity of residual CIP and its decomposition products after the ozone treatment.

The MIC values of the CIP solution before ozone treatment in the APO and FO systems were 0.043 and 0.035 g/mL against *E. coli* and 0.093 and 0.085 g/mL against *S. aureus*, as presented in Fig. S7 and Tables S3–S5. The CIP solution after treatment in the APO system showed no antimicrobial activity even when the dose of CIP administered was increased to 0.9 g/mL. In contrast, the FO system still showed an inhibition activity when the administered CIP was 0.073 and 0.58 g/mL for *E. coli* and *S. aureus*, respectively, as shown in Figure 8. These results confirm that the residual CIP and its decomposition products from in the APO system were 12 and 1.5 times less toxic against *E. coli* and *S. aureus* as compared with those resulted in the FO system. This provides an interpretation that ozone attacked the piperazinyl moiety of CIP [54], which is responsible for its antibacterial activity against both Gram-negative and Gram-positive bacteria [72]. The amplification of CIP biodegradability allows ozone to break down CIP into smaller molecules [73]. The elimination of the carboxyl groups as well as oxidation of the fluorine group of quinolone, which are the moieties that play important roles in the binding process to the DNA gyrase enzyme of the target protein to inhibit microbial proliferation [59, 72, 74] are believed to be the reasons for the decreasing antimicrobial activity of CIP [54].

It is also noteworthy that the piperazinyl moiety of CIP has a large electron density, making it susceptible to being attacked by free radicals such as  $\text{OH}^{\bullet}$ ,  $\text{O}_2^{\bullet-}$ , and  $\text{HO}_2^{\bullet}$  [26, 49, 65]. In many reports, these ROS would likely attack the fluorine group first through substitution or hydrolysis reactions [33, 54, 65], although the cleavage of the C–F bond in

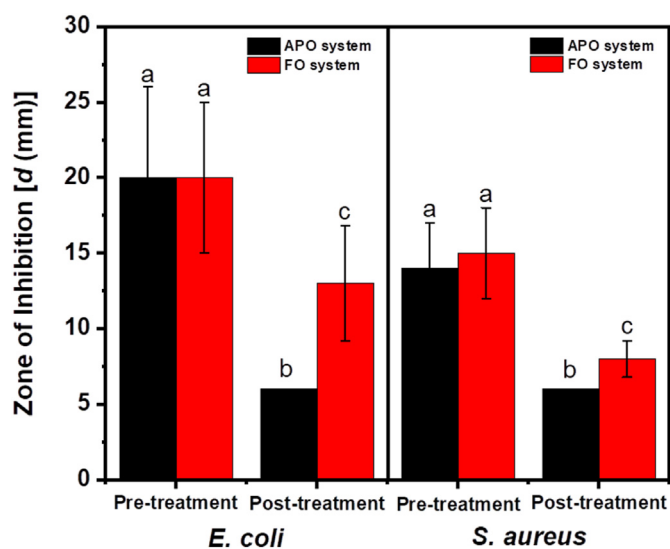
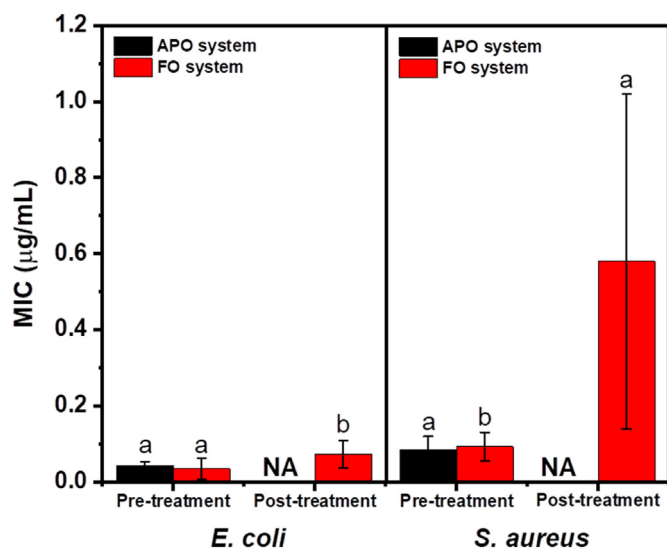


Figure 7. The diameter of growth inhibition zone,  $d$  (mm), of *E. coli* and *S. aureus* bacterial strains by ciprofloxacin solution before and after being treated with ozone microbubbles generated through the APO system and the FO system.



**Figure 8.** The MIC towards *E. coli* and *S. aureus* of ciprofloxacin solution before and after being treated with ozone microbubbles before and after being treated with ozone microbubbles generated through the APO system and the FO system.

the fluorine group requires more energy than those needed to break the C–H or C–N bonds [33]. These are due to both OH<sup>−</sup> and O<sub>3</sub> having high oxidation potentials of 2.7 and 2.08 V, respectively. Substitution reactions of the fluorine group by a hydroxyl compound or hydroxylation could also occur, as it has been proposed by Sarangapani et al. [54]. This direct attack of the piperazinyl moiety of CIP tends to involve a high potential oxidizing agent to degrade this compound, which is known to have a mechanism of steric hindrance [75, 76].

#### 4. Conclusion

In conclusion, a comparative study of the degradation of ciprofloxacin (CIP) using ozone microbubbles injected via the conventional diffusion (FO) system and the aerator pump (APO) systems has been investigated. Overall the performance of the APO system was better than the FO system based on all tested parameters. While the mechanism of degradation of CIP by ozone treatment is generally attributed to the oxidation reaction of the antibiotic with reactive oxygen species, such as hydroxyl, oxygen, and hydroperoxyl radicals, generated on the surface of ozone microbubbles, it was shown that the introduction of an in-house aerator pump design significantly enhanced the efficiency and efficacy of ozonation in the degradation of fused-ring antibiotics such as CIP. The rate and efficiency of degradation of CIP were estimated to be  $3.64 \times 10^{-3}$ /min and 83.5% using the APO system, higher compared with those of the FO system, where the degradation rate and efficiency were  $1.47 \times 10^{-3}$ /min and 60.9%, respectively. The enhanced degradation efficiency of CIP by the APO system was also revealed by its higher electrical energy efficiency (0.146 g/kWh), compared to that of the FO system (0.106 g/kWh). These results are in line with the lower antibacterial activity and minimum inhibition concentration of the remaining CIP and its by-products in the solution, against both *E. coli* and *S. aureus* bacteria, after being treated with the APO system compared with the FO system. Overall findings confirmed that the introduction of an aerator pump in the APO system generated higher population of smaller sized microbubbles, which proportionally improve degradation efficiency of CIP, compared with the diffused injection of the FO system. The results presented in this work opened up a vista for advanced degradation of pharmaceutical contaminants such as CIP using ozone microbubbles. However, the method could be further developed to generate more ozone microbubbles and nanobubbles, and to reduce the number of macrobubbles. In addition, further investigation is necessary to analyze the

removal of antibiotics using ozone microbubbles where other organic contaminants are present in the wastewater as these organic contaminants may compete as scavengers for the ROS generated in the wastewater.

#### Declarations

##### Author contribution statement

Sera Budi Verinda, Muflihathul Muniroh, Eko Yulianto, Nani Maharani: Performed the experiments.

Gunawan Gunawan, Nur Farida Amalia: Contributed reagents, materials, analysis tools or data.

Jonathan Hobley, Anwar Usman: Analyzed and interpreted the data; Wrote the paper.

Muhammad Nur: Conceived and designed the experiments; Analyzed and interpreted the data.

##### Funding statement

This work was supported by Universitas Diponegoro, Indonesia through the PMDSU Research Funding Program (No. 14-10/UN7.P4.3/PP/2020).

##### Data availability statement

Data included in article/supplementary material/referenced in article.

##### Declaration of interests statement

The authors declare no conflict of interest.

##### Additional information

Supplementary content related to this article has been published online at <https://doi.org/10.1016/j.heliyon.2022.e10137>.

##### Acknowledgements

Authors would like to acknowledge the supports given by research assistants of Centre for Plasma Research and Microbiology Laboratory of the Faculty of Medicine of Universitas Diponegoro. JH is grateful to National Cheng Kung University's NCKU90 distinguished visiting scholar program for hosting his research.

##### References

- [1] E.Y. Klein, T.P. Van Boeckel, E.M. Martinez, S. Pant, S. Gandra, S.A. Levin, H. Goossens, R. Laxminarayan, Global increase and geographic convergence in antibiotic consumption between 2000 and 2015, *Proc. Natl. Acad. Sci. U. S. A.* 115 (2018) E3463–E3470.
- [2] S.I. Polianciuc, A.E. Gurzău, B. Kiss, M.G. Ştefan, F. Loghin, Antibiotics in the environment: causes and consequences, *Med. Pharm. Rep.* 93 (2020) 231–240.
- [3] M.C. Danner, A. Robertson, V. Behrends, J. Reiss, Antibiotic pollution in surface fresh waters: occurrence and effects, *Sci. Total Environ.* 664 (2019) 793–804.
- [4] M. Kumar, S. Jaiswal, K.K. Sodhi, P. Shree, D.K. Singh, P.K. Agrawal, P. Shukla, Antibiotics bioremediation: perspectives on its ecotoxicity and resistance, *Environ. Int.* 124 (2019) 448–461.
- [5] J. Wang, L. Chu, L. Wojnárovits, E. Takács, Occurrence and fate of antibiotics, antibiotic resistant genes (ARGs) and antibiotic resistant bacteria (ARB) in municipal wastewater treatment plant: an overview, *Sci. Total Environ.* 744 (2020), 140997.
- [6] S. Rodríguez-Mozaz, I. Vaz-Moreira, S. Varela Della Giustina, M. Llorca, D. Barceló, S. Schubert, T.U. Berendonk, I. Michael-Kordatou, D. Fatta-Kassinos, J.L. Martinez, C. Elpers, I. Henriques, T. Jaeger, T. Schwartz, E. Paulshus, K. O'Sullivan, K.M.M. Pärnänen, M. Virta, T.T. Do, F. Walsh, C.M. Manaia, Antibiotic residues in final effluents of European wastewater treatment plants and their impact on the aquatic environment, *Environ. Int.* 140 (2020), 105733.

- [7] A.S. Adeleye, J. Xue, Y. Zhao, A.A. Taylor, J.E. Zenobio, Y. Sun, Z. Han, O.A. Salawu, Y. Zhu, Abundance, fate, and effects of pharmaceuticals and personal care products in aquatic environments, *J. Hazard Mater.* 424 (2022), 127284.
- [8] J.M. Blondeau, Fluoroquinolones: mechanism of action, classification, and development of resistance, *Surv. Ophthalmol.* 49 (2004) 1–6.
- [9] D.J. Smart, H.D. Halicka, F. Traganos, Z. Darzynkiewicz, G.M. Williams, Ciprofloxacin-induced G2 arrest and apoptosis in TK6 lymphoblastoid cells is not dependent on DNA double-strand break formation, *Cancer Biol. Ther.* 7 (2008) 113–119.
- [10] V. Yadav, P. Talwar, Repositioning of fluoroquinolones from antibiotic to anti-cancer agents: an underestimated truth, *Biomed. Pharmacother.* 111 (2019) 934–946.
- [11] F.Y. Bai, S. Ni, Y.Z. Tang, X.M. Pan, Z. Zhao, Ciprofloxacin transformation in aqueous environments: mechanism, kinetics, and toxicity assessment during •OH-mediated oxidation, *Sci. Total Environ.* 699 (2020), 134190.
- [12] B. Nas, T. Dolu, S. Koyuncu, Behavior and Removal of ciprofloxacin and sulfamethoxazole antibiotics in three different types of full-scale wastewater treatment plants: a comparative study, *Water Air Soil Pollut.* 232 (2021) 127.
- [13] L. Huang, Y. Mo, Z. Wu, S. Rad, X. Song, H. Zeng, S. Bashir, B. Kang, Z. Chen, Occurrence, distribution, and health risk assessment of quinolone antibiotics in water, sediment, and fish species of Qingshitan reservoir, South China, *Sci. Rep.* 10 (2020), 15777.
- [14] S.W. Hyung, J. Lee, S.Y. Baek, S. Lee, J. Han, B. Kim, K.H. Choi, S. Ahn, D.K. Lim, H. Lee, Method improvement for analysis of enrofloxacin and ciprofloxacin in chicken meat: application of in-sample addition of trace ethylenediaminetetraacetic acid to isotope dilution ultra-performance liquid chromatography–mass spectrometry, *Chromatographia* 85 (2022) 35–45.
- [15] S. Keerthanan, C. Jayasinghe, J.K. Biswas, M. Vithanage, Pharmaceutical and Personal Care Products (PPCPs) in the environment: plant uptake, translocation, bioaccumulation, and human health risks, *Crit. Rev. Environ. Sci. Technol.* 51 (2021) 1221–1258.
- [16] F.V. Mello, S.C. Cunha, F.H.S. Fogaça, M.B. Alonso, J.P.M. Torres, J.O. Fernandes, Occurrence of pharmaceuticals in seafood from two Brazilian coastal areas: implication for human risk assessment, *Sci. Total Environ.* 803 (2022), 149744.
- [17] R. Widiastuti, E. Martindah, Y. Anastasia, Detection and dietary exposure assessment of fluoroquinolones residues in chicken meat from the district of Malang and Blitar, Indonesia, *Trop. Anim. Sci. J.* 45 (2022) 98–103.
- [18] I.C. Stanton, A.K. Murray, L. Zhang, J. Snape, W.H. Gaze, Evolution of antibiotic resistance at low antibiotic concentrations including selection below the minimal selective concentration, *Commun. Biol.* 3 (2020) 467.
- [19] W. Nabgan, M. Saeed, A.A. Jalil, B. Nabgan, Y. Gambo, M.W. Ali, M. Ikram, A. Kadier, M.Y. Mohamad, A state of the art review on electrochemical technique for the remediation of pharmaceuticals containing wastewater, *Environ. Res.* 210 (2022), 112975.
- [20] L.F. Zhai, H.Y. Guo, Y.Y. Chen, M. Sun, S. Wang, Structure-dependent degradation of pharmaceuticals and personal care products by electrocatalytic wet air oxidation: a study by computational and experimental approaches, *Chem. Eng. J.* 423 (2021), 130167.
- [21] D. Palomares-Reyna, J.E. Carrera-Crespo, F.S. Sosa-Rodríguez, U.M. García-Pérez, I. Fuentes-Camargo, L. Lartundo-Rojas, J. Vazquez-Arenas, Photo-electrochemical and ozonation process to degrade ciprofloxacin in synthetic municipal wastewater, using C, N-codoped TiO<sub>2</sub> with high visible-light absorption, *J. Environ. Chem. Eng.* 10 (2022), 107380.
- [22] R. Noroozi, M. Gholami, M. Farzadkia, A.J. Jafari, Degradation of ciprofloxacin by CuFe<sub>2</sub>O<sub>4</sub>/GO activated PMS process in aqueous solution: performance, mechanism and degradation pathway, *Int. J. Environ. Anal. Chem.* 102 (2020) 174–195.
- [23] J. Fick, H. Söderström, R.H. Lindberg, C. Phan, M. Tysklind, D.G.J. Larsson, Pharmaceuticals and personal care products in the environment: contamination of surface, ground, and drinking water from pharmaceutical production, *Environ. Toxicol. Chem.* 28 (2009) 2522–2527.
- [24] M.A.F. Locatelli, F.F. Sodrè, W.F. Jardim, Determination of antibiotics in Brazilian surface waters using liquid chromatography–electrospray tandem mass spectrometry, *Arch. Environ. Contam. Toxicol.* 60 (2011) 385–393.
- [25] D.B. Miklos, C. Remy, M. Jekel, K.G. Linden, J.E. Drewes, U. Hübner, Evaluation of advanced oxidation processes for water and wastewater treatment – a critical review, *Water Res.* 139 (2018) 118–131.
- [26] K. Shang, R. Morent, N. Wang, Y. Wang, B. Peng, N. Jiang, N. Lu, J. Li, Degradation of sulfamethoxazole (SMX) by water falling film DBD Plasma/Persulfate: reactive species identification and their role in SMX degradation, *Chem. Eng. J.* 431 (2022), 133916.
- [27] S. Iqbal, I. Bibi, F. Majid, K. Jillani, S. Kamal, M. Iqbal, S. Ata, N. Nazar, H. Albalawi, N. Alwadai, The electrochemical, dielectric, and ferroelectric properties of Gd and Fe doped LaNiO<sub>3</sub> with an efficient solar-light driven catalytic activity to oxidize malachite green dye, *J. Colloid Interface Sci.* 607 (2022) 568–583.
- [28] Y. Zeng, D. Chen, T. Chen, M. Cai, Q. Zhang, Z. Xie, R. Li, Z. Xiao, G. Liu, W. Lv, Study on heterogeneous photocatalytic ozonation degradation of ciprofloxacin by TiO<sub>2</sub>/carbon dots: kinetic, mechanism and pathway investigation, *Chemosphere* 227 (2019) 198–206.
- [29] J. Cheng, D. Wang, B. Wang, H. Ning, Y. Zhang, Y. Li, J. An, P. Gao, Plasma-catalytic degradation of ciprofloxacin in aqueous solution over different MnO<sub>2</sub> nanocrystals in a dielectric barrier discharge system, *Chemosphere* 253 (2020), 126595.
- [30] H. Li, T. Li, S. He, J. Zhou, T. Wang, L. Zhu, Efficient degradation of antibiotics by non-thermal discharge plasma: highlight the impacts of molecular structures and degradation pathways, *Chem. Eng. J.* 395 (2020), 125091.
- [31] R.C. Sanito, S.-J. You, Y.-F. Wang, Degradation of contaminants in plasma technology: an overview, *J. Hazard Mater.* 424 (2022), 127390.
- [32] E.M. Cuerda-correa, M.F. Alexandre-franco, C. Fern, Advanced oxidation processes for the removal of antibiotics from water, An overview, *Water* 12 (2020) 1–50.
- [33] J. Deng, G. Wu, S. Yuan, X. Zhan, W. Wang, Z.-H. Hu, Ciprofloxacin degradation in UV/chlorine advanced oxidation process: influencing factors, mechanisms and degradation pathways, *J. Photochem. Photobiol., A: Chem* 371 (2019) 151–158.
- [34] S.G. Michael, I. Michael-Kordatou, S. Nahim-Granados, M.I. Polo-López, J. Rocha, A.B. Martínez-Piernas, P. Fernández-Ibáñez, A. Agüera, C.M. Manaia, D. Fatta-Kassinos, Investigating the impact of UV-C/H<sub>2</sub>O<sub>2</sub> and sunlight/H<sub>2</sub>O<sub>2</sub> on the removal of antibiotics, antibiotic resistance determinants and toxicity present in urban wastewater, *Chem. Eng. J.* 388 (2020), 124383.
- [35] A. Sheikhmohammadi, E. Asgari, B. Hashemzadeh, Photo-catalytic degradation of ciprofloxacin by UV/ZnO/SO<sub>3</sub> process: performance, kinetic, degradation pathway, energy consumption and total cost of system, *Int. J. Environ. Anal. Chem.* (2022) in the press.
- [36] R. Sander, Compilation of Henry's law constants (version 4.0) for water as solvent, *Atmos. Chem. Phys.* 15 (2015) 4399–4981.
- [37] A. John, A. Brookes, I. Carra, B. Jefferson, P. Jarvis, Microbubbles and their application to ozonation in water treatment: a critical review exploring their benefit and future application, *Crit. Rev. Environ. Sci. Technol.* 52 (2022) 1561–1603.
- [38] W. Fan, W.-G. An, M.-X. Huo, W. Yang, S.-Y. Zhu, S.-S. Lin, Solubilization and stabilization for prolonged reactivity of ozone using micro-nano bubbles and ozone-saturated solvent: a promising enhancement for ozonation, *Separ. Purif. Technol.* 238 (2020), 116484.
- [39] A. Gurung, O. Dahl, K. Jansson, The fundamental phenomena of nanobubbles and their behavior in wastewater treatment technologies, *Geosystem Eng* 19 (2016) 133–142.
- [40] K. Yao, Y. Chi, F. Wang, J. Yan, M. Ni, K. Cen, The effect of microbubbles on gas-liquid mass transfer coefficient and degradation rate of COD in wastewater treatment, *Water Sci. Technol.* 73 (2016) 1969–1977.
- [41] T. Zheng, Q. Wang, T. Zhang, Z. Shi, Y. Tian, S. Shi, N. Smale, J. Wang, Microbubble enhanced ozonation process for advanced treatment of wastewater produced in acrylic fiber manufacturing industry, *J. Hazard Mater.* 287 (2015) 412–420.
- [42] M. Nur, A.I. Susan, Z. Muhlisin, F. Arianto, A.W. Kinandana, I. Nurhasanah, S. Sumariyah, P.J. Wibawa, G. Gunawan, A. Usman, Evaluation of novel integrated dielectric barrier discharge plasma as ozone generator, *Bull. Chem. React. Eng. Catal.* 12 (2017) 24–31.
- [43] M. Nur, E. Yulianto, A.W. Kinandana, M. Restiwijaya, F. Arianto, Development of DDBD and plasma jet reactors for production reactive species plasma chemistry, *IOP Conf. Ser. Mater. Sci. Eng.* 509 (2019), 012086.
- [44] P. Li, Development of Advanced Water Treatment Technology Using Microbubbles, Keio Univ, Japan, 2006. PhD Diss.
- [45] P. Li, M. Takahashi, K. Chiba, Enhanced free-radical generation by shrinking microbubbles using a copper catalyst, *Chemosphere* 77 (2009) 1157–1160.
- [46] U. Chasanah, E. Yulianto, A.Z. Zain, E. Sasmita, M. Restiwijaya, A.W. Kinandana, F. Arianto, M. Nur, Evaluation of titration method on determination of ozone concentration produced by dielectric barrier discharge plasma (DBDP) technology, *J. Phys.: Conf. Ser.* 1153 (2019), 012086.
- [47] C.A. Sennoga, E. Kanbar, A. Bouakaz, An ImageJ Plugin for the Sizing and Counting of Microbubbles, IEEE Int. Ultrason. Symp., Taipei, Taiwan, 2015.
- [48] M. Ansari, A.H. Mahvi, M.H. Salmani, M. Sharifian, H. Fallahzadeh, M.H. Ehrampoush, Dielectric barrier discharge plasma combined with nano catalyst for aqueous amoxicillin removal: performance modeling, kinetics and optimization study, energy yield, degradation pathway, and toxicity, *Separ. Purif. Technol.* 251 (2020), 117270.
- [49] T. Ahamad, M. Naushad, S.M. Alshehri, Analysis of degradation pathways and intermediates products for ciprofloxacin using a highly porous photocatalyst, *Chem. Eng. J.* 417 (2021), 127969.
- [50] K.F. Christodoulis, M.A. Theodoropoulou, C.D. Tsakiroglou, Remediation of oil-drilling cuttings by ozonation in semibatch bubble column reactors, *IOP Conf. Ser. Earth Environ. Sci.* 899 (2021), 012066.
- [51] F. Gelman, R. Binstock, L. Halicz, Application of the Walkley-Black titration for the organic carbon quantification in organic rich sedimentary rocks, *Fuel* 96 (2012) 608–610.
- [52] The European Committee on Antimicrobial Susceptibility Testing, Reading Guide: EUCAST Disk Diffusion Method for Antimicrobial Susceptibility Testing, 2021, Version 3.0.
- [53] I. Wiegand, K. Hilpert, R.E.W. Hancock, Agar and broth dilution methods to determine the minimal inhibitory concentration (MIC) of antimicrobial substances, *Nat. Protoc.* 3 (2008) 163–175.
- [54] C. Sarangapani, D. Zuzina, P. Behan, D. Boehm, B.F. Gilmore, P.J. Cullen, P. Bourke, Degradation kinetics of cold plasma-treated antibiotics and their antimicrobial activity, *Sci. Rep.* 9 (2019) 1–15.
- [55] A.K. Bin, Ozone dissolution in aqueous systems treatment of the experimental data, *Exp. Therm. Fluid Sci.* 28 (2004) 395–405.
- [56] H. Oliveira, A. Azevedo, J. Rubio, Nanobubbles generation in a high-rate hydrodynamic cavitation tube, *Miner. Eng.* 116 (2018) 32–34.
- [57] S. Nazari, S.Z. Shafaei, A. Hassanzadeh, A. Azizi, M. Gharabaghi, R. Ahmadi, B. Shahbazi, Study of effective parameters on generating submicron (nano)-bubbles using the hydrodynamic cavitation, *Physicochem. Probl. Miner. Process.* 56 (2020) 884–904.
- [58] Z. Pourkarimi, B. Rezaei, M. Noaparast, A.V. Nguyen, S. Chehreh Chelgani, Proving the existence of nanobubbles produced by hydrodynamic cavitation and their significant effects in powder flotation, *Adv. Powder Technol.* 32 (2021) 1810–1818.
- [59] C. Wang, C.-Y. Lin, G.-Y. Liao, Degradation of antibiotic tetracycline by ultraviolet-bubble ozonation process, *J. Water Proc. Eng.* 37 (2020), 101463.

- [60] G.V. Egorova, V.A. Voblikova, L.V. Sabitova, I.S. Tkachenko, S.N. Tkachenko, V.V. Lunin, Ozone solubility in water, *Moscow Univ. Chem. Bull.* 70 (2015) 207–210.
- [61] D. Gardoni, A. Vailati, R. Canziani, Decay of ozone in water: a review, *Ozone Sci. Eng.* 34 (2012) 233–242.
- [62] C.A. Aggelopoulos, S. Meropoulos, M. Hatzisymeon, Z.G. Lada, G. Rassias, Degradation of antibiotic enrofloxacin in water by gas-liquid nsp-DBD plasma: parametric analysis, effect of H<sub>2</sub>O<sub>2</sub> and CaO<sub>2</sub> additives and exploration of degradation mechanisms, *Chem. Eng. J.* 398 (2020), 125622.
- [63] H.M. Jalali, Kinetic study of antibiotic ciprofloxacin ozonation by MWCNT/MnO<sub>2</sub> using Monte Carlo simulation, *Mater. Sci. Eng. C* 59 (2016) 924–929.
- [64] T. Azuma, K. Otomo, M. Kunitou, M. Shimizu, K. Hosomaru, S. Mikata, Y. Mino, T. Hayashi, Removal of pharmaceuticals in water by introduction of ozonated microbubbles, *Separ. Purif. Technol.* 212 (2019) 483–489.
- [65] E.A. Serna-Galvis, F. Ferraro, J. Silva-Agredo, R.A. Torres-Palma, Degradation of highly consumed fluoroquinolones, penicillins and cephalosporins in distilled water and simulated hospital wastewater by UV254 and UV254/persulfate processes, *Water Res.* 122 (2017) 128–138.
- [66] L.W. Gassie, J.D. Englehardt, Mineralization of greywater organics by the ozone-UV advanced oxidation process: kinetic modeling and efficiency, *Environ. Sci. Water Res. Technol.* 5 (2019) 1956–1970.
- [67] L. Luo, D. Zou, D. Lu, B. Xin, M. Zhou, X. Zhai, J. Ma, Heterogeneous catalytic ozonation of ciprofloxacin in aqueous solution using a manganese-modified silicate ore, *RSC Adv.* 8 (2018) 33534–33541.
- [68] M.R.K. Kashani, R. Kiani, A. Hassani, A. Kadier, S. Madihi-Bidgoli, K.-Y.A. Lin, F. Ghanbari, Electro-peroxone application for ciprofloxacin degradation in aqueous solution using sacrificial iron anode: a new hybrid process, *Separ. Purif. Technol.* 292 (2022), 121026.
- [69] R. Xu, L. Li, X. Fu, L. Yu, Y. Jin, L. Li, Catalytic ozonation of ciprofloxacin with Cu–Al layered double hydroxides based on response surface analysis, *J. Environ. Eng.* 148 (2022) 1–10.
- [70] S. Aleksić, A.Ž. Gotvajn, K. Premzl, M. Kolar, S.Š. Turk, Ozonation of amoxicillin and ciprofloxacin in model hospital wastewater to increase biotreatability, *Antibiotics (Basel)* 10 (2021) 1407.
- [71] S. Khuntia, S.K. Majumder, P. Ghosh, Quantitative prediction of generation of hydroxyl radicals from ozone microbubbles, *Chem. Eng. Res. Des.* 98 (2015) 231–239.
- [72] T.D.M. Pham, Z.M. Ziora, M.A.T. Blaskovich, Quinolone antibiotics, *Medchemcomm* 10 (2019) 1719–1739.
- [73] S. Mohan, P. Balakrishnan, Kinetics of ciprofloxacin removal using a sequential two-step ozonation-biotreatment process, *Environ. Technol. Innovat.* 21 (2021), 101284.
- [74] J.M. Domagala, Review: structure-activity and structure-side effect relationships for the quinolone antibacterials, *J. Antimicrob. Chemother.* 33 (1994) 685–706.
- [75] M.F. Da Silva, I. Tiago, A. Veríssimo, R.A. Boaventura, O.C. Nunes, C.M. Manaia, Antibiotic resistance of enterococci and related bacteria in an urban wastewater treatment plant, *FEMS Microbiol. Ecol.* 55 (2006) 322–329.
- [76] E.A. Auerbach, E.E. Seyfried, K.D. McMahon, Tetracycline resistance genes in activated sludge wastewater treatment plants, *Water Res.* 41 (2007) 1143–1151.